Regular Article

blood

MYELOID NEOPLASIA

LXR agonist treatment of blastic plasmacytoid dendritic cell neoplasm restores cholesterol efflux and triggers apoptosis

Adam Ceroi,[1-4] David Masson,[4,5] Anne Roggy,[1-4] Christophe Roumier,[6] Cécile Chagué,[1-4] Thierry Gauthier,[1-4] Laure Philippe,[1-4] Baptiste Lamarthée,[1-4] Fanny Angelot-Delettre,[1-4] Francis Bonnefoy,[1-4] Sylvain Perruche,[1-4] Sabeha Biichle,[1-3] Claude Preudhomme,[6] Elisabeth Macintyre,[7] Laurent Lagrost,[4,5] Francine Garnache-Ottou,[1-4] and Philippe Saas[1-4]

[1]Unité 1098, INSERM, Besançon, France; [2]Université Bourgogne Franche-Comté, Unité Mixte de Recherche 1098, Besançon, France; [3]Etablissement Français du Sang Bourgogne Franche-Comté, Besançon, France; [4]Laboratoires d'Excellence (LabEx) Lipoprotéines et Santé: Prévention et Traitement des Maladies Inflammatoires et du Cancer (LipSTIC), Besançon/Dijon, France; [5]Faculté de Médecine, Université Bourgogne Franche-Comté, INSERM Unité 866, Dijon, France; [6]Laboratoire d'Hématologie, Centre de Biologie Pathologie, Institut de Recherches sur le Cancer de Lille, Centre Hospitalier Régional Universitaire de Lille, INSERM Unité 837, Lille, France; and [7]Laboratoire d'Onco-Hématologie, Hôpital Necker-Enfants Malades, Assistance Publique–Hôpitaux de Paris, Faculté de Médecine Descartes, Université Sorbonne Paris Cité, INSERM Unité 1151, Paris, France

Key Points

- LXR activation inhibits BPDCN cell survival through the increase of cholesterol efflux, the inhibition of NF-κB, and IL-3 signaling.
- Treatment with LXR agonists can be proposed as a new therapeutic approach for BPDCN.

Blastic plasmacytoid dendritic cell (PDC) neoplasm (BPDCN) is an aggressive hematological malignancy with a poor prognosis that derives from PDCs. No consensus for optimal treatment modalities is available today and the full characterization of this leukemia is still emerging. We identified here a BPDCN-specific transcriptomic profile when compared with those of acute myeloid leukemia and T-acute lymphoblastic leukemia, as well as the transcriptomic signature of primary PDCs. This BPDCN gene signature identified a dysregulation of genes involved in cholesterol homeostasis, some of them being liver X receptor (LXR) target genes. LXR agonist treatment of primary BPDCN cells and BPDCN cell lines restored LXR target gene expression and increased cholesterol efflux via the upregulation of adenosine triphosphate–binding cassette (ABC) transporters, ABCA1 and ABCG1. LXR agonist treatment was responsible for limiting BPDCN cell proliferation and inducing intrinsic apoptotic cell death. LXR activation in BPDCN cells was shown to interfere with 3 signaling pathways associated with leukemic cell survival, namely: NF-κB activation, as well as Akt and STAT5 phosphorylation in response to the BPDCN growth/survival factor interleukin-3. These effects were increased by the stimulation of cholesterol efflux through a lipid acceptor, the apolipoprotein A1. In vivo experiments using a mouse model of BPDCN cell xenograft revealed a decrease of leukemic cell infiltration and BPDCN-induced cytopenia associated with increased survival after LXR agonist treatment. This demonstrates that cholesterol homeostasis is modified in BPDCN and can be normalized by treatment with LXR agonists which can be proposed as a new therapeutic approach. (*Blood*. 2016;128(23):2694-2707)

Introduction

Blastic plasmacytoid dendritic cell (PDC) neoplasm (BPDCN) is a rare aggressive malignancy derived from PDCs.[1] This disease is characterized by a heterogeneous presentation at diagnosis (from a disease limited to the skin to a leukemic syndrome with cytopenia and bone marrow involvement), clinical heterogeneity, and manifestations easily changing during disease progression.[2] Currently, there is no consensus regarding the optimal treatment modality.[2] Most BPDCN patients have a very aggressive clinical course with limited median overall survival.[2,3] It has been recently proposed that the frequent relapse after treatment and the poor prognosis can be related to the fact that the involvement of the central nervous system (CNS) is frequently undetected.[4] Recently, BPDCN was classified by the World Health Organization (WHO) as a distinct entity in the group of "acute myeloid leukemia (AML) and related precursor neoplasms."[2,5] Extensive characterization of this malignancy is still limited and diagnosis overlap may exist with immature AML, monoblastic and undifferentiated leukemia. Thus, a better understanding of this leukemia and new therapeutic approaches are urgently needed.

Previous studies have identified a cholesterol metabolism dysregulation in different malignant cells leading to intracellular cholesterol accumulation.[6,7] Cellular cholesterol content results from cholesterol uptake and biosynthesis through the mevalonate pathway, while its

Submitted 27 June 2016; accepted 19 September 2016. Prepublished online as *Blood* First Edition paper, 4 October 2016; DOI 10.1182/blood-2016-06-724807.

The data reported in this article have been deposited in the Gene Expression Omnibus database (accession numbers GSM705329 to GSM705333, and GSE89565).

The online version of this article contains a data supplement.

The publication costs of this article were defrayed in part by page charge payment. Therefore, and solely to indicate this fact, this article is hereby marked "advertisement" in accordance with 18 USC section 1734.

© 2016 by The American Society of Hematology

Downloaded from http://ashpublications.net/blood/article-pdf/128/23/2694/1396962/blood724807.pdf by guest on 03 June 2024

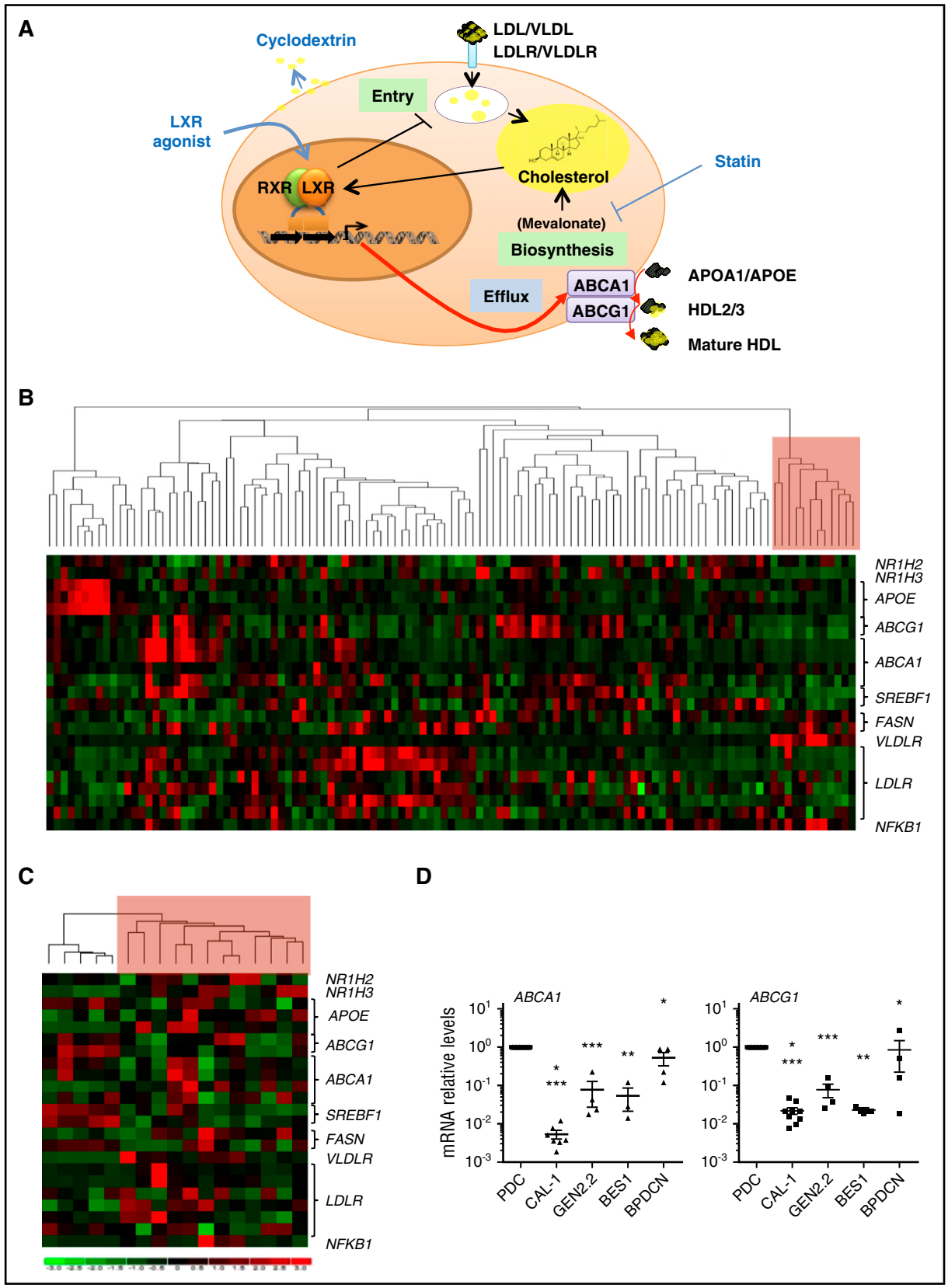

Figure 1. A BPDCN-specific transcriptomic signature with a dysregulation of genes involved in cholesterol homeostasis allows the clustering of BPDCN samples. (A) A schematic representation of cellular cholesterol homeostasis. Mechanisms of cholesterol synthesis and uptake (green boxes) and efflux (blue box) maintain cellular cholesterol homeostasis. The LXR pathway is involved in the regulation of cholesterol homeostasis by inhibiting cholesterol uptake/entry (through the decreased expression of low-density lipoprotein (LDL) and/or very-low-density lipoprotein (VLDL) receptors, LDLR and VLDLR, respectively) and by stimulating cholesterol efflux (through ABC transporters, ABCA1 and ABCG1). This LXR pathway is activated by intermediates from the mevalonate pathway (ie, the cholesterol biosynthesis). Cholesterol efflux also requires cholesterol acceptors, APOA1/APOE, and HDL2/3 to form mature HDL. These cholesterol acceptors can be provided by the cell itself or represent circulating

Downloaded from http://ashpublications.net/blood/article-pdf/128/23/2694/1396962/blood724807.pdf by guest on 03 June 2024

elimination is mediated by cholesterol efflux (Figure 1A). Cholesterol uptake involves plasma lipoproteins (mainly LDL and VLDL) after interactions with their specific receptors, LDLR and VLDLR, respectively. Cholesterol efflux implicates mainly adenosine triphosphate–binding cassettes (ABCs) A1 and G1 (ABCA1 and ABCG1, respectively) in association with extracellular cholesterol acceptors, including: apolipoprotein A1/E (APOA1 and APOE, respectively) or lipoprotein particles (eg, nascent high-density lipoprotein [HDL] or HDL2).[8]

Leukemic cells (AML and chronic myeloid leukemia) have been shown to increase LDLR expression,[6] decrease LDLR degradation,[7] and stimulate cholesterol biosynthesis resulting in cholesterol accumulation.[6] Cholesterol regulates critical cellular functions, including plasma membrane formation, fluidity, and permeability.[9] These latter functions are implicated in survival signaling pathway activation (eg, Akt)[10] and proliferation.[11,12] For instance, stimulation of cholesterol efflux inhibits interleukin-3 (IL-3)-induced hematological progenitor cell proliferation.[13,14] Interestingly, BPDCN cells express high levels of IL-3 receptor α chain (CD123), and IL-3 is a BPDCN survival factor.[1,15] A targeted therapy directed against IL-3 receptor, called SL-401 associating IL-3 with the catalytic and translocation domains of diphteria toxin, has been tested in a phase 1/2 study with encouraging results.[16,17] Whether cholesterol homeostasis is dysregulated in BPDCN and contributes to its aggressiveness or determines response to therapies remains to be determined.

Cholesterol homeostasis is regulated at least by liver X receptors (LXRs). These nuclear receptors are expressed as 2 isoforms, with LXRβ being the ubiquitous isoform whereas LXRα expression is restricted to cells with high cholesterol turnover (eg, hepatocytes or macrophages).[18,19] The LXR pathway is activated by intermediates from the mevalonate pathway, endogenous oxidized cholesterol derivatives (called oxysterols), and synthetic agonists (eg, T0901317 or GW3965).[19,20] These synthetic compounds are of great interest for therapeutic use because LXR are considered as a promising target in different diseases.[19-21] LXR activation upregulates the expression of several genes involved in cholesterol homeostasis (called LXR target genes), including: *ABCA1*, *ABCG1*,[21] and *APOE* (related to cholesterol efflux),[22] as well as the "inducible degrader of the low-density lipoprotein receptor" preventing cholesterol uptake through LDLR/VLDLR degradation.[23,24] Overall, these mechanisms participate in decreased intracellular cholesterol content. LXRs are functionally expressed in normal PDCs and in a leukemic PDC cell line,[25] but no data are available on the effects of LXR agonists on BPDCN.

The goal of this study was to determine whether BPDCN exhibit a specific gene signature based on genes involved in cholesterol efflux and uptake, in comparison with other leukemic cells (AML and T-acute lymphoblastic leukemia [T-ALL]) and normal PDCs. Because LXR activation controls cholesterol homeostasis via LXR target genes, we studied whether LXR agonist treatment stimulates cholesterol efflux. Effects of LXR activation on cell proliferation and survival were evaluated in vitro, using primary BPDCN samples and 2 established BPDCN cell lines (CAL-1 and GEN2.2). The in vivo LXR agonist therapeutic effect was evaluated using a BPDCN xenograft model treated with the T0901317 LXR agonist.

Methods

BPDCN collection

Twenty-three BPDCN samples were obtained at diagnosis (sample collection authorization number DC-2008-713). BPDCN was diagnosed based on histopathology and immunostaining of cutaneous lesions, blood, or bone marrow samples, as described.[26-28] This study was approved by our local ethics committee (Comité de Protection des Personnes [CPP] Est II, Besançon, France).

Cell lines and culture

Two established BPDCN cell lines (CAL-1 and GEN2.2),[29,30] primary BPDCN cells isolated from a patient and expanded in NOD-SCID IL2Rγc-deficient (NSG) mice (The Jackson Laboratory, Sacramento, CA) (referred to hereafter as BES1), as well as 11 BPDCN samples with different BPDCN infiltration (supplemental Table 1, available on the *Blood* Web site) from newly diagnosed patients were used for in vitro assays. Culture of BPDCN cells and isolation of primary BPDCN samples are described in supplemental Methods.

Transcriptomic analysis

The following samples were submitted to transcriptomic analysis using the GeneChip Human Genome U133 Plus 2.0 Array (Affymetrix, Santa Clara, CA):

- 12 BPDCN samples,
- 65 AML samples (including different French-American-British subtypes: 25 M0, 11 M1, 10 M2, 1 M3, 11 M4, 6 M5, and 1 M6) (Unité 837, Institut de Recherches sur le Cancer de Lille [IRCL], Lille, France),
- 35 T-ALL samples (Unité 1151, Assistance Publique–Hôpitaux de Paris [AP-HP], Hôpital Necker-Enfants Malades, Paris, France) (available at https://www.dropbox.com/sh/v21hg015hf515gw/AAC63OgjzcXXqTM-myca5sjVca?dl=0), and
- 5 primary PDCs (available on the Gene Expression Omnibus [GEO] database, under recording numbers: GSM705329, GSM705330, GSM705331, GSM705332, GSM705333).

Data were analyzed using dChip software (http://www.softpedia.com/get/Science-CAD/dChip.shtml) based on the expression of cholesterol homeostasis and LXR-related genes (*LXRA*, *LXRB*, *ABCA1*, *ABCG1*, *APOE*, *SREBF1*, *FASN*, *LDLR*, and *VLDLR*) plus the *NFKB1* gene.

Quantitative RT-PCR analysis

Transcription of LXR target genes (*ABCA1*, *ABCG1*) and genes coding proteins involved in the intrinsic apoptosis (*BCL2*, *BAK1*, *BAX*) was evaluated by quantitative reverse transcription polymerase chain reaction (qRT-PCR), as described.[25] Details are given in supplemental Methods.

Cholesterol efflux assay

CAL-1 cells were used to assess cholesterol efflux, as described in supplemental Methods and in Ishibashi et al.[31]

Figure 1 (continued) apolipoproteins or lipoprotein particles. Molecules used to modify cholesterol homeostasis in BPDCN are indicated in blue font. (B) Transcriptomic analysis of 65 AML, 35 T-ALL, and 12 BPDCN samples (highlighted in red, right side of the panel) was performed using an Affymetrix U133-2 chip and dChip software. (C) Transcriptomic analysis of the 12 BPDCN samples was compared with 5 primary PDC samples obtained using an Affymetrix U133-2 chip and dChip software. (D) Basal LXR target gene (*ABCA1*, *ABCG1*) transcripts were quantified by qRT-PCR in 2 established BPDCN cell lines, CAL-1 (n = 7) and GEN2.2 cells (n = 4), as well as in a short-term BPDCN cell line, BES1 (n = 3) and 4 primary BPDCN samples (leukemic PDC [LPDC] #2-4, and #7, n = 1). Levels of mRNA were normalized to those of glyceraldehyde-3-phosphate dehydrogenase (GAPDH) for each sample and then expressed as fold change relative to the average value for normal PDCs. Results from n independent experiments with each symbol representing an experiment (*$P < .05$, **$P < .01$, ****$P < .0001$, Mann-Whitney). FASN, fatty acid synthase; RXR, retinoid X receptor.

Downloaded from http://ashpublications.net/blood/article-pdf/128/23/2694/1396962/blood724807.pdf by guest on 03 June 2024

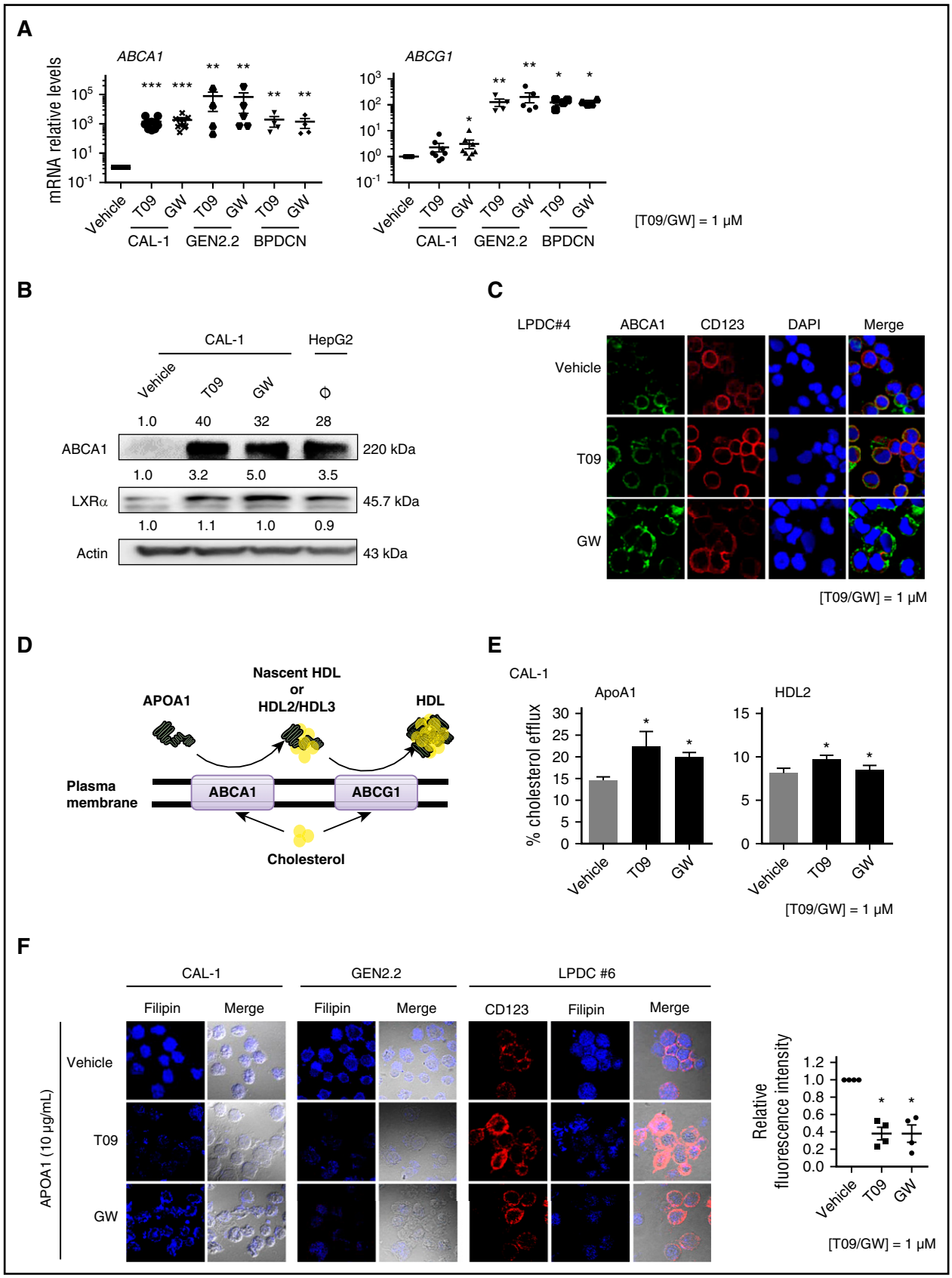

Figure 2. LXR activation restores cholesterol homeostasis-related gene expression and induces cholesterol efflux from BPDCN. (A) BPDCN cell lines (CAL-1, GEN2.2) and blood samples from 4 patients diagnosed with BPDCN (LPDC #4, #7, #8, #10) were treated with 1 µM LXR agonists, T0901317 (T09) or GW3965 (GW), for 24 hours. *ABCA1* and *ABCG1* mRNA levels were determined by qRT-PCR in CAL-1 (n = 8), GEN2.2 (n = 5), and in blood samples containing >75% of leukemic PDCs (n = 4). Levels of mRNA were normalized to those of *GAPDH* for each sample and then expressed as fold change relative to the average value for vehicle-treated cells (*$P < .05$,

Downloaded from http://ashpublications.net/blood/article-pdf/128/23/2694/1396962/blood724807.pdf by guest on 03 June 2024

Flow cytometry

Cytotoxic effects of LXR agonists were evaluated by staining with Annexin V (AnxV) and 7-amino-actinomycin D (7AAD) (fluorescein isothiocyanate–conjugated AnxV/7AAD; BD Biosciences, Le Pont de Claix, France) or caspase-9 activation (CaspGLOW Fluorescein Active Caspase Staining kit; eBioscience), according to the manufacturer's instructions. Proliferation was assessed on CAL-1 cells after labeling with the cell proliferation dye, eFluor 450 (eBioscience SA, Paris, France). BPDCN gating was performed using antibodies against CD123, CD131, and CD304 (supplemental Table 3). Cell cycle analysis was performed after cell fixation in ethanol 70% (overnight, 4°C), and by propidium iodide staining in a solution containing RNAse (overnight, 4°C). Cell fluorescence was evaluated using a CANTO II cytometer (BD Biosciences, San Jose, CA) and DIVA 6.2 software (BD Biosciences), except for cell cycle analysis where a FC500 cytometer with CXP and WinCycle softwares (Beckman Coulter Immunotech, Miami, FL) were used.

Immunoblotting

Whole-cell protein fraction was obtained by cell lysis in Laemmli buffer (supplemental Methods). Nuclear and cytosolic fractions were separated by cell lysis using a hypotonic, and then hypertonic, buffer solution (for osmosis restauration, supplemental Methods). Cytosolic fraction was isolated by centrifugation while nuclei were lysed in Laemmli buffer. Proteins were separated by electrophoresis on 8.5% or 12% sodium dodecyl sulfate–polyacrylamide gels and transferred to polyvinylidene difluoride membranes (GE Healthcare). Blots were then saturated with 5% milk before incubation with specific antibodies (supplemental Table 3). Blotted proteins were detected and quantified on a bioluminescence imager and BIO-1D advanced software (Vilber-Lourmat, Marne-la-Vallée, France) after blots were incubated with a horseradish peroxidase–conjugated appropriate secondary antibody. Details on blot saturation and quantification are given in supplemental Methods.

Confocal microscopy

Protein expression (CD123 and ABCA1) and phosphorylation (p65, STAT5, and Akt) were evaluated by immunofluorescent staining, as previously described[25] (antibodies used appear in supplemental Table 3). Nuclei were labeled with 4′,6-diamidino-2-phenylindole (DAPI; Sigma-Aldrich) and cholesterol content was investigated using the free cholesterol marker filipin (Sigma-Aldrich), according to the manufacturer's recommendations. Relative fluorescence intensity of filipin staining was measured with the ImageJ application, and determined as: corrected total cell fluorescence = [“integrated density” − (“area of selected cell” × “mean fluorescence of background readings”)]/untreated conditions.

Mice and in vivo model

NSG mice were irradiated (2 Gy), inoculated IV 18 hours later with 1×10^6 CAL-1 cells, and treated intraperitoneally 7 days later with 6 injections of T0901317 (total experimental dose, 30 or 60 mg/kg, respectively) or with dimethyl sulfoxide (DMSO)/phosphate-buffered saline (PBS) control solution. Mouse monitoring and quantification of BPDCN cell infiltrate were described in supplemental Methods. Experimentation (#11007R) was approved by our local ethics committee (#58, approved by the French Ministry of Higher Education and Research) and conducted in accordance with the European Union Directive 2010/63.

Statistical analysis

Statistical analyses were performed by GraphPad Prism version 6 (GraphPad Software, San Diego, CA), using the Mann-Whitney, Wilcoxon, or Mantel-Cox test (*$P < .05$, **$P < .01$, ***$P < .001$, ****$P < .0001$). Data are expressed as mean ± standard error of the mean (SEM).

Results

A BPDCN-specific transcriptomic signature identifies a dysregulation of cholesterol homeostasis

Twelve primary BPDCN samples were analyzed using the Affymetrix U133-2 messenger RNA (mRNA) microarray for the expression of cholesterol homeostasis and LXR-related genes (*LXRA*, *LXRB*, *ABCA1*, *ABCG1*, *APOE*, *SREBF1*, *FASN*, *LDLR*, and *VLDLR*) plus the *NFKB1* gene. Comparison with AML and T-ALL samples revealed a specific BPDCN sample clustering, associated with a significant downregulation of LXR target genes *ABCA1* and *ABCG1* (associated with cholesterol efflux) and an upregulation of the *VLDLR* gene (linked to cholesterol entry). *NFKB1* gene upregulation in BPDCN samples was confirmed (Figure 1B; supplemental Figure 1).[32] Comparison of the BPDCN samples with primary PDC samples showed a similar clustering associated with a significant downregulation of LXR target genes, *SREBF1* and *ABCG1*, whereas *VLDLR* and *NFKB1* genes were upregulated (Figure 1C; supplemental Figure 1). This shows that the BPDCN transcriptomic profile is independent of the PDC cell lineage. A significant downregulation of *ABCA1* and *ABCG1* gene transcription was confirmed by qRT-PCR analysis in 2 BPDCN cell lines (GEN2.2 and CAL-1), BES1 cells, and 4 primary BPDCN samples compared with nonleukemic PDC samples (Figure 1D). Overall, these data identify a specific perturbation of cholesterol homeostasis- and LXR-related gene transcription in BPDCN.

LXR activation stimulates cholesterol efflux from BPDCN

Treatment with 2 synthetic LXR agonists (T0901317 and GW3965, 1 μM, 24 hours) upregulated *ABCA1* and *ABCG1* gene transcription in CAL-1, GEN2.2 cell lines, and in 4 primary BPDCN samples (Figure 2A). ABCA1 and LXRα proteins were increased after LXR activation in CAL-1 cells, as assessed by western blot analysis (Figure 2B) and in CAL-1 and GEN2.2 cells, as assessed by confocal

Figure 2 (continued) **$P < .01$, ****$P < .0001$, Mann-Whitney). (B) CAL-1 cells were treated with 1 μM T0901317 (T09) or GW3965 (GW), or vehicle control alone, for 24 hours. LXRα isoform and ABCA1 protein expression were evaluated by western blot. The human hepatocellular carcinoma cell line HepG2 was used as control and reference for LXRα and ABCA1 expression, whereas untreated CAL-1 lysates were used as reference for actin expression. Expression of LXR protein was compared with actin expression with the vehicle condition being considered arbitrary as 1. Results of 1 experiment of 3 are shown. (C) Primary BPDCN cells from 1 patient (LPDC #4) were treated with 1 μM LXR agonists T0901317 (T09) or GW3965 (GW) for 24 hours. Expression of CD123 (as a BPDCN-specific marker) and ABCA1 was assessed by confocal microscopy. Nuclei were stained with DAPI. (D) This cartoon, adapted from Oram and Vaughan,[8] represents 1 of the current accepted models of cholesterol efflux, illustrating cholesterol efflux experiments performed thereafter. Cholesterol is excluded from cells through ABCA1 and/or ABCG1 transporters. Lipid-poor APOA1 accepts cholesterol (yellow symbols) from cells through ABCA1-mediated cholesterol efflux. This induces nascent HDL formation which then accepts supplemental cholesterol loading via ABCG1-mediated efflux. Addition of HDL2 implicates only ABCG1-mediated cholesterol efflux. (E) Cholesterol efflux was assessed using [^{3}H]-cholesterol-acetylated LDL-loaded CAL-1 cells treated with 1 μM T0901317 (T09) or GW3965 (GW) for 24 hours. Cholesterol efflux was triggered by the addition of 20 μg/mL HDL2 (right panel, n = 4) or 10 μg/mL APOA1 (left panel, n = 3). Data were expressed as percentage of cholesterol efflux (mean ± SEM of n experiments), as described in supplemental Methods (*$P < .05$, Mann-Whitney). (F) Cholesterol content of BPDCN cells was assessed after treatment with T0901317 (T09) or GW3965 (1 μM) for 24 hours followed by a 4-hour incubation with APOA1 cholesterol acceptor (10 μg/mL). Cellular cholesterol content was determined using filipin staining analyzed by confocal microscopy. One representative experiment of 3 for CAL-1 cells, 1 of 2 for GEN2.2 cells, is shown. LPDC represents data of a blood sample from 1 BPDCN patient tested of 4 (LPDC #5, #6, #8, #9). The PDC marker CD123 allows the identification of leukemic PDCs in blood samples. Cumulative filipin fluorescence intensity from the 4 different BPDCN samples was expressed as mean ± SEM (bottom right panel, *$P < .05$, Mann-Whitney). Fluorescence intensity of the vehicle condition is considered arbitrary as 1.

Downloaded from http://ashpublications.net/blood/article-pdf/128/23/2694/1396962/blood724807.pdf by guest on 03 June 2024

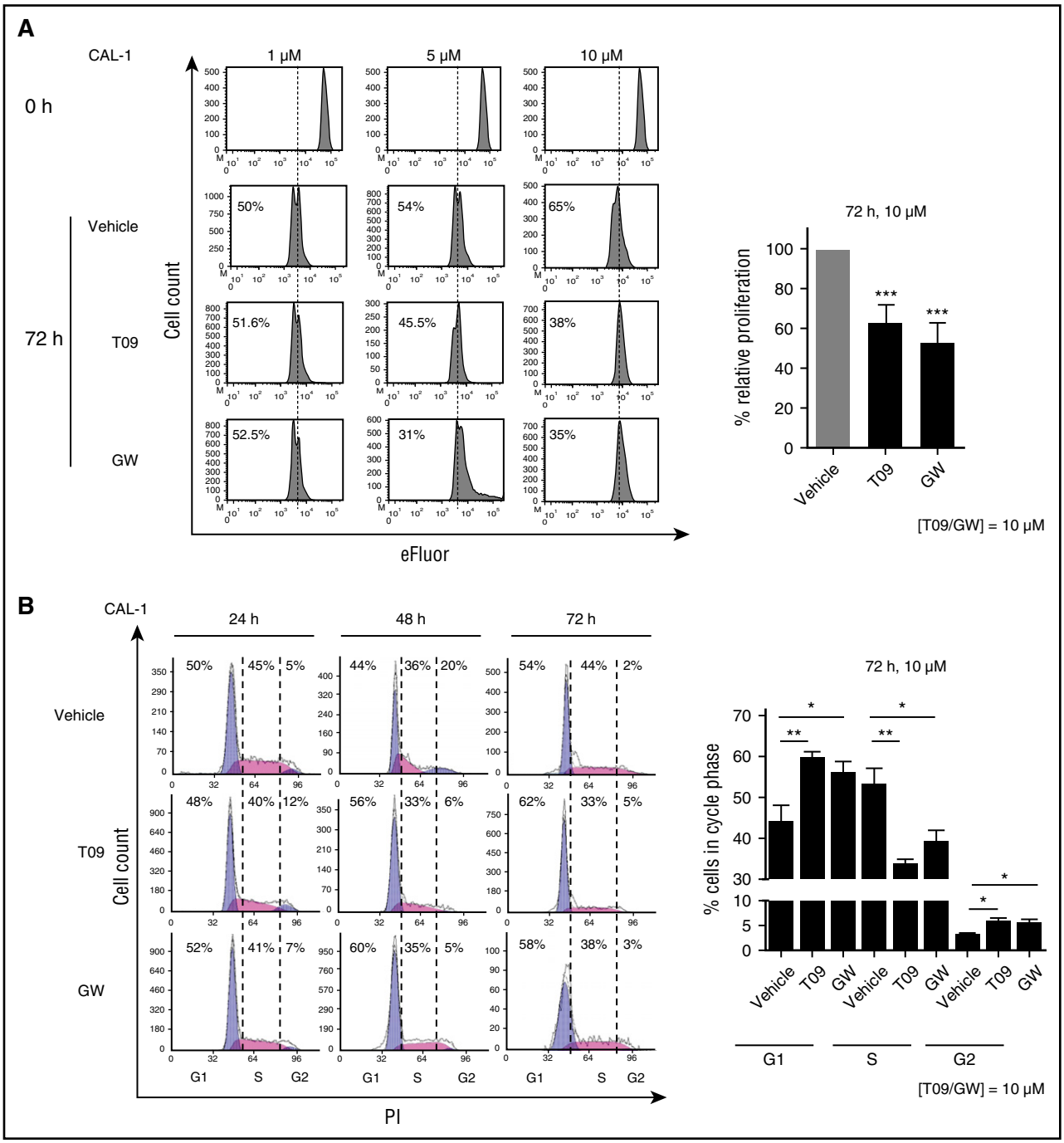

Figure 3. LXR activation inhibits BPDCN cell proliferation. (A) Left panel, eFluor-labeled CAL-1 cells were treated with increasing noncytotoxic concentrations (1 μM, 5 μM, and 10 μM) of LXR agonists, T0901317 (T09) or GW3965 (GW), for 72 hours. Cell proliferation was assessed by eFluor dilution analyzed by flow cytometry. Histograms show 1 representative experiment of 10. Right panel, Cumulative data from the 10 independent experiments are expressed as relative proliferation (mean ± SEM) with the vehicle condition being considered as 100%. Data depicted for LXR agonist treatment illustrate the highest concentration, 10 μM T0901317 (T09) or GW3965 (GW) (***$P < .001$, Wilcoxon). (B) Left panel, CAL-1 cells were treated with 10 μM T09, GW, or vehicle control for 24, 48, or 72 hours. Cell cycle phase distribution was assessed by cytometry (n = 5). Right panel, Cumulative data from 5 independent experiments are expressed as percentage of cells in each cell cycle phase (mean ± SEM) for the highest concentration of LXR agonists, 10 μM (*$P < .05$, **$P < .01$,***$P < .001$, Wilcoxon). PI, propidium iodide.

microscopy (supplemental Figure 2). Increase of ABCA1 expression after LXR activation was analyzed in 1 primary BPDCN sample by confocal microscopy (Figure 2C). Because LXR activation induces cholesterol efflux through ABCA1 and ABCG1 in cooperation with cholesterol acceptors, such as APOA1 and HDL2,[8,21] we then investigated cholesterol efflux using CAL-1 cells preloaded with ^{3}H-cholesterol (1 μCi/mL, 24 hours), and treated with either T0901317 or GW3965 (1 μM, 24 hours) before the addition of APOA1 (10 μg/mL) or HDL2 (20 mg of protein per mL) cholesterol acceptors for 4 hours (Figure 2D). Radioactivity measurement in media and cells demonstrated that LXR agonist treatment significantly increased cholesterol efflux in both conditions (Figure 2E). Intracellular cholesterol staining revealed that LXR agonist treatment followed by APOA1 addition induced a significant diminution of total cholesterol content in CAL-1,

Downloaded from http://ashpublications.net/blood/article-pdf/128/23/2694/1396962/blood724807.pdf by guest on 03 June 2024

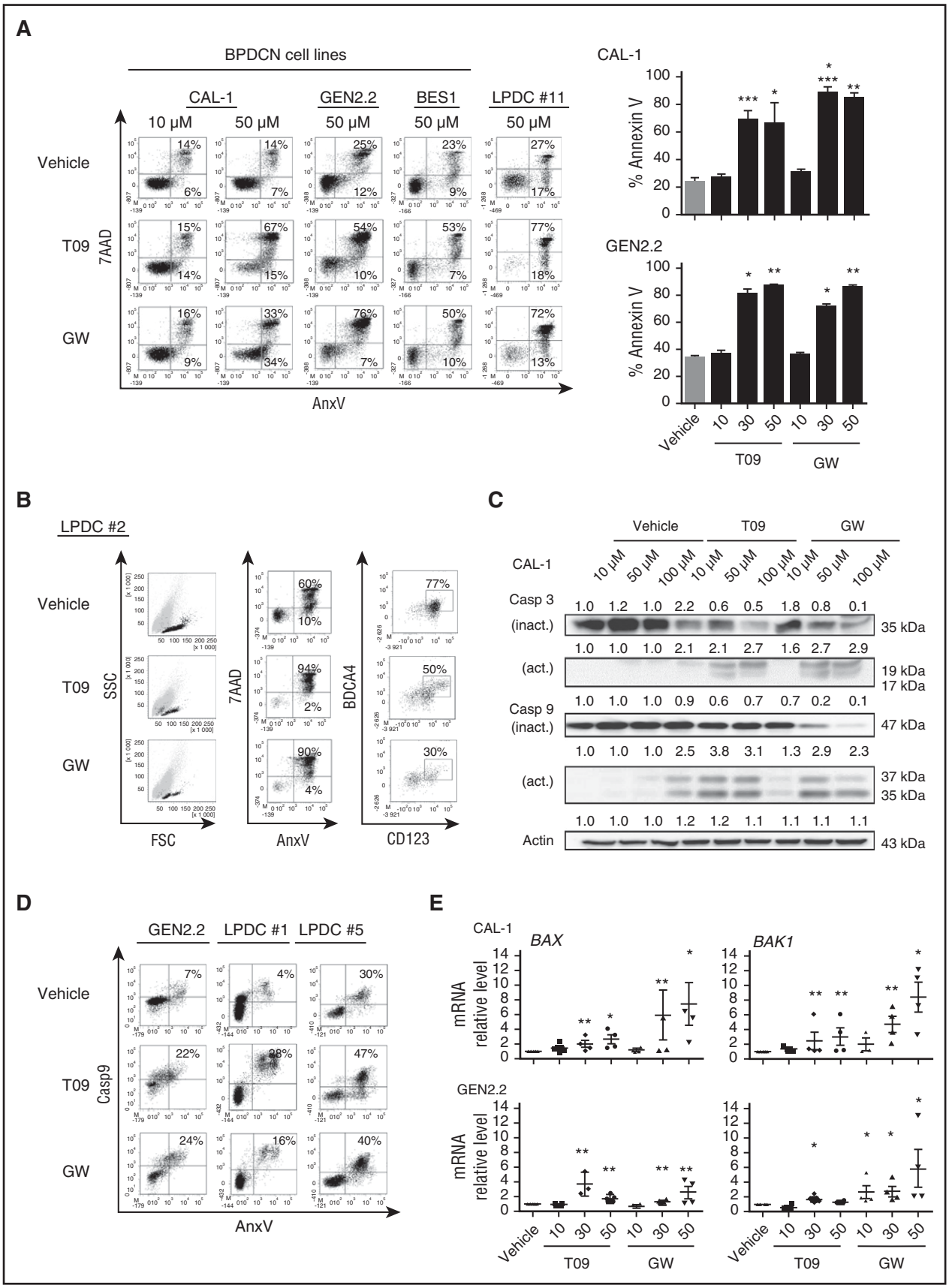

Figure 4. LXR activation in BPDCN cells induces apoptotic cell death. CAL-1, GEN2.2, BES1, and blood samples from 5 patients diagnosed with BPDCN (LPDC #1, #2, #5, #10, #11) were treated with increasing concentrations (10-50 µM) of LXR agonists T0901317 (T09) or GW3965 (GW) for 24 hours. Cell viability was assessed by AnxV and 7AAD staining and cytometry. (A) Left panel, Dot plots illustrate data obtained with cells treated with 50 µM LXR agonists, except for CAL-1 cells that were treated with

Downloaded from http://ashpublications.net/blood/article-pdf/128/23/2694/1396962/blood724807.pdf by guest on 03 June 2024

GEN2.2 cells, and in 4 primary BPDCN samples (*$P < .05$), as assessed by confocal microscopy (Figure 2F). Overall, these data demonstrated that LXR agonist treatment of BPDCN stimulates cholesterol efflux via ABCA1 and ABCG1 transporters.

LXR activation inhibits BPDCN cell proliferation and induces apoptotic cell death

Because LXR activation regulates cell proliferation and survival,[13,20] we investigated the effects of LXR stimulation on BPDCN cells. CAL-1 cells were treated with increasing concentrations (1 μM, 5 μM, 10 μM) of LXR agonists for 24, 48, or 72 hours. Proliferation analysis of viable cells ($AnxV^-/7AAD^-$) demonstrated a significant decrease of cell proliferation induced by LXR agonist treatment (10 μM, 72 hours, $P < .001$), as assessed by cytometry (Figure 3A). Cell cycle phase analysis demonstrated a significant G1 phase retention associated with a diminution of cells in the S phase in a time-dependent (24 or 72 hours) manner (Figure 3B).

Exposure of CAL-1 and GEN2.2 cells to increasing concentrations of LXR agonists (10 μM, 30 μM, or 50 μM) demonstrated a significant cell death induction for concentrations higher than 10 μM, as assessed by AnxV/7AAD staining and cytometry. The cytotoxic effect of LXR agonists was confirmed in BES1 cells and 5 primary BPDCN samples of 5 tested ($P < .05$; Figure 4A-B). Assessment of viable BPDCN cells ($AnxV^-/7AAD^-/CD123^+/CD304^+$) in 1 blood sample from a BPDCN patient revealed after treatment with LXR agonists, a preferential decrease of viable BPDCN cells (77% vs 50% and 30%, for vehicle- vs T0901317- and GW3965-treated samples, respectively) (Figure 4B). This suggests a specific cytotoxic effect of LXR agonists on BPDCN cells. Western blot analysis of CAL-1 cells treated with LXR agonists for 6 hours showed a caspase-3 and caspase-9 cleavage, suggesting apoptosis induction (Figure 4C). This was confirmed in CAL-1 and GEN2.2 cells by nucleus fragmentation induced by LXR agonists and at morphological levels, as assessed by confocal microscopy (supplemental Figure 3A-B). Caspase-9 activation was confirmed after LXR agonist treatment in GEN2.2 cells and 2 primary BPDCN cells, as assessed by cytometry (Figure 4D). BAX- and BAK1-coding gene upregulation in CAL-1 and GEN2.2 cells after LXR activation was detected (Figure 4E). This suggests the involvement of the intrinsic apoptosis. Overall, this indicated that LXR agonist treatment stimulates apoptotic cell death in BPDCN.

LXR activation interferes with 2 BPDCN survival pathways: the IL-3–induced signaling pathway and NF-κB activation

Because LXR activation inhibits BPDCN survival, we wondered whether LXR stimulation would interfere with the following survival signaling pathways, IL-3 and NF-κB. IL-3 was described to induce STAT5 and Akt activation, both involved in leukemic cell survival.[33-36] NF-κB activation was reported to maintain BPDCN cell survival.[32] To investigate the effects of LXR activation on IL-3–induced STAT5 and Akt activation, CAL-1 cells were treated with increasing noncytotoxic concentrations of LXR agonists (1-10 μM, 24 hours), followed by IL-3 stimulation (10 ng/mL, 30 minutes). Western blot analysis demonstrated a sustained diminution of STAT5 and Akt phosphorylation induced by LXR agonist treatment (Figure 5A). These effects were confirmed by confocal microscopy in 3 primary BPDCN samples (Figure 5B), as well as in CAL-1 and GEN2.2 cells (supplemental Figure 4A).

To demonstrate the involvement of constitutive NF-κB activation in BPDCN cell survival, CAL-1 and GEN2.2 cells were treated with increasing concentrations (12.5-100 μM, 24 hours) of the NF-κB p65 inhibitor, JSH23. A significant increase of BPDCN cell death was revealed by AnxV/7AAD staining (**$P < .01$, Figure 5C). LXR agonists decreased NF-κB p65 phosphorylation in 4 primary BPDCN samples (Figure 5D) and in CAL-1, GEN2.2 cells (supplemental Figure 4B), as assessed by confocal microscopy. Western blot analysis of CAL-1 cells pretreated with LXR agonists (1 μM, 24 hours) demonstrated an inhibition of p50, p65, and c-Rel NF-κB subunit nuclear translocation, induced by a NF-κB activator (R848, 1 μg/mL, 6 hours) (Figure 5E). Overall, these data demonstrated that LXR stimulation in BPDCN cells inhibits IL-3–induced STAT5 and Akt activation, as well as NF-κB activation at phosphorylation and nuclear translocation levels. This may contribute to the cytotoxic effects of LXR agonist treatment on BPDCN.

Stimulation of cholesterol efflux amplifies LXR activation-induced effects

Cholesterol efflux through ABCA1/ABCG1 inhibits IL-3–induced hematopoietic stem cell (HSC) proliferation,[13,14] and LXR activation in BPDCN interferes with the IL-3 signaling pathway. To investigate the contribution of LXR-stimulated cholesterol efflux in these effects, CAL-1 and GEN2.2 cells or a primary BPDCN sample were treated with LXR agonists (1 μM, 24 hours), then with APOA1 (10 μg/mL, 4 hours) followed by IL-3 (10 ng/mL, 30 minutes). Addition of APOA1 markedly diminished IL-3–induced STAT5 and Akt phosphorylation in all LXR-treated BPDCN cells (Figure 6A-B). Treatment of CAL-1 cells with increasing noncytotoxic concentrations of LXR agonists (5-10 μM) in the presence of APOA1 (0-20 μg/mL) showed a significant increase of dead BPDCN cells (Figure 6C). Overall, these data demonstrated that cholesterol efflux increases LXR agonist-mediated effects. To go further on cholesterol dependency of BPDCN, cholesterol was deprived from BPDCN cells by using either an inhibitor of the mevalonate pathway, atorvastatin, or a compound inducing cholesterol removal from cells, methyl-β-cyclodextrin.[37] Cell death analysis 24 hours later by AnxV/7AAD staining and cytometry demonstrated a significant BPDCN cell death (supplemental Figure 5).

Figure 4 (continued) 10 μM and 50 μM. Results from 1 representative experiment of 6 for CAL-1, 1 of 4 for GEN2.2 cells, and 1 representative sample (LPDC#11) of 5 for primary BPDCN samples tested. Right panel, The percentage of $AnxV^+$ dead cells (mean ± SEM from 6 or 4 independent experiments for CAL-1 and GEN2.2, respectively), after LXR agonist treatment (*$P < .05$, **$P < .01$, ***$P < .001$, ****$P < .0001$, Mann-Whitney). (B) One freshly isolated blood sample obtained from a patient diagnosed with BPDCN was treated with 50 μM T0901317 (T09) or GW3965 (GW) for 24 hours. Cytometry dot plots from 1 representative sample of 5 different BPDCN represent the percentage of BPDCN cells (identified by CD123/BDCA4 staining) in the viable cell fraction of blood sample (ie, the $AnxV^-/7AAD^-$ fraction) (*$P < .05$, Mann-Whitney). (C) CAL-1 cells were treated with increasing concentrations of LXR agonists, T0901317 (T09) or GW3965 (GW), for 6 hours. Analysis of full-length inactive (inact.) and cleaved active (act.) forms of caspase-3 and caspase-9 was performed by western blot. Expression of these proteins was compared with actin expression with the vehicle condition being considered as 1. Results from 1 representative experiment of 3. (D) BPDCN cells (GEN2.2 and 2 primary BPDCN samples, LPDC #1 and #5) were treated with 50 μM T0901317 (T09) or GW3965 (GW) for 6 hours. Caspase-9 activation on $7AAD^-$ cell fraction (excluding late apoptotic and necrotic cells) was assessed by cytometry. One dot plot represents 1 representative experiment of 2 for GEN2.2 cells, and the other 2 dot plots represent the experiments performed on 2 BPDCN samples (LPDC #1 and #5). (E) CAL-1 and GEN2.2 cells were treated with increasing concentrations of LXR agonists (10 μM, 30 μM, and 50 μM) for 6 hours. *BCL2*, *BAX*, and *BAK1* gene expression was assessed by qRT-PCR. Levels of mRNA were normalized to those of *GAPDH* for each sample and then expressed as fold change related to the average value for vehicle-treated cells. Cumulative data from 4 independent experiments expressed as mean ± SEM (*$P < .05$, **$P < .01$, Mann-Whitney) are shown. FSC, forward scatter; SSC, side scatter.

Downloaded from http://ashpublications.net/blood/article-pdf/128/23/2694/1396962/blood724807.pdf by guest on 03 June 2024

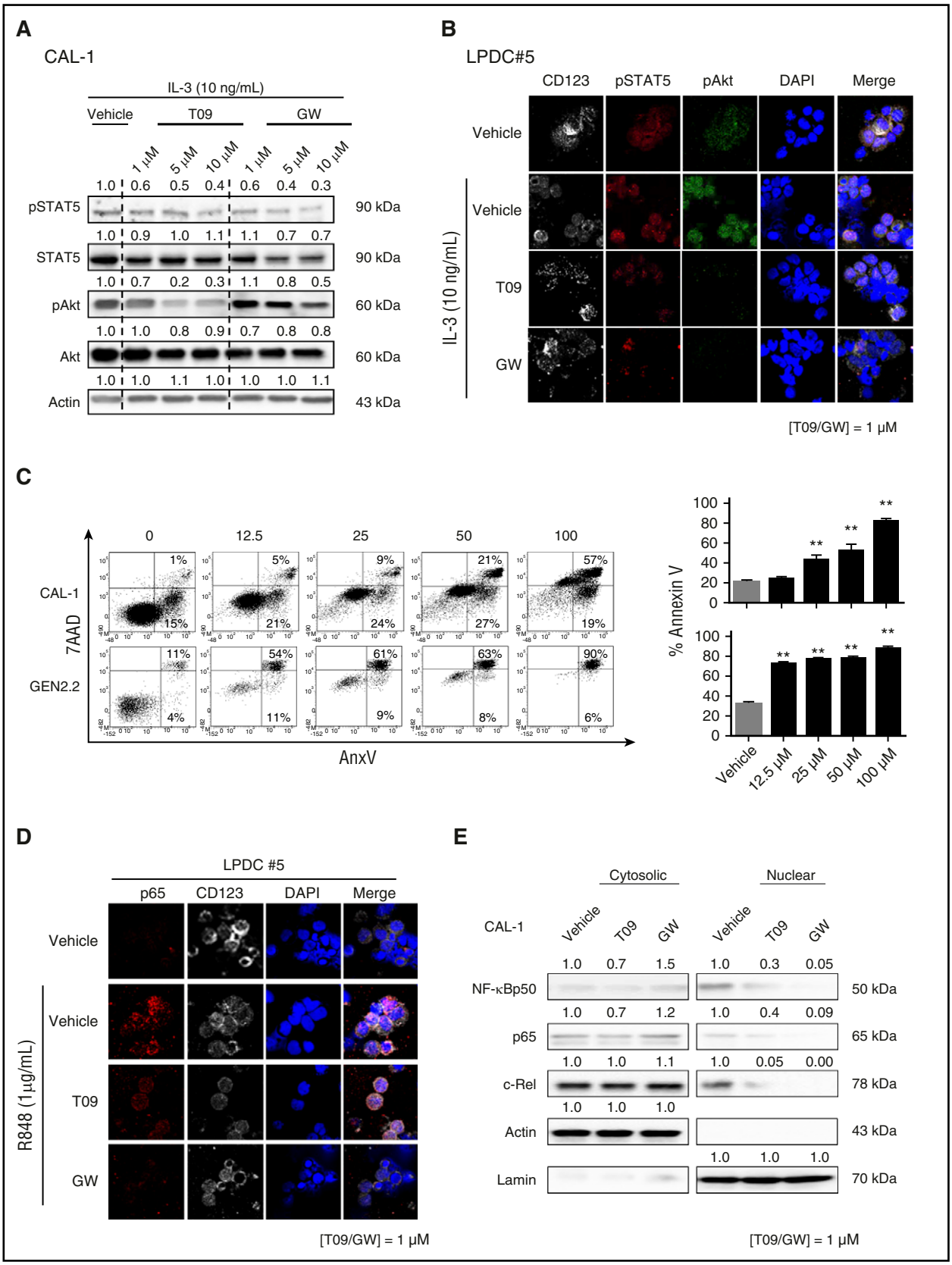

Figure 5. LXR activation in BPDCN cells interferes with IL-3–induced STAT5 and Akt phosphorylation, as well as NF-κB activation. (A) CAL-1 cells were treated with increasing concentrations (1 μM, 5 μM, or 10 μM) of LXR agonists (T09 or GW) for 24 hours, followed by 10 ng/mL of IL-3 for 30 minutes. Phospho-STAT5 (Y694), phospho-Akt (S473), as well as unphosphorylated corresponding protein expression was assessed by western blot. The expression of these proteins was compared with actin with the vehicle condition being considered as 1. Results of 1 representative experiment of 2. (B) BPDCN cells (LPDC #5) were treated with 1 μM LXR agonists for 24 hours. Phospho-STAT5 (Y694) and phospho-Akt (S473) were assessed by confocal microscopy after IL-3 stimulation (10 ng/mL, 30 minutes). Results of 1 representative sample (LPDC #5) of

Downloaded from http://ashpublications.net/blood/article-pdf/128/23/2694/1396962/blood724807.pdf by guest on 03 June 2024

In vivo LXR agonist treatment prevents cytopenia and BPDCN cell infiltration

To assess LXR therapeutic effects in vivo, sublethally irradiated (2 Gy) NSG mice were grafted with 1 million CAL-1 cells. After 7 days, mice were treated with 2 doses of LXR agonist (T0901317 30 mg/kg or 60 mg/kg) or vehicle, every 2 days until sacrifice. Although CAL-1 cell injection induced a significant persistent decrease of red blood cell (RBC), platelet counts, as well as hemoglobin (Hb) concentration, T0901317-treated mice showed a significant prevention of cytopenia, including RBC counts and Hb concentration (Figure 7A). At sacrifice, a diminution of CAL-1 cell-induced splenomegaly was observed (Figure 7B), supported by a potent decrease of spleen and bone marrow BPDCN cell infiltration, as assessed by flow cytometry (Figure 7C). In an additional experiment, treatment with T0901317 (30 mg/kg or 60 mg/kg) significantly increased the overall survival of NSG mice inoculated with CAL-1 cells compared with CAL-1-inoculated and vehicle-treated mice (Figure 7D-E). Overall, these data provide the in vitro and in vivo demonstration of a therapeutic effect of LXR agonist on BPDCN through different mechanisms, including signaling pathway regulation and cholesterol efflux.

Discussion

Cholesterol is a critical component for cell growth and proliferation, as illustrated by the inhibition of HSC proliferation occurring after cholesterol efflux through ABC transporters.[13,14] In physiological conditions, cholesterol homeostasis is tightly controlled by the LXR signaling pathway. Here, we identified that the aggressive hematological malignancy BPDCN exhibits a specific transcriptomic signature with a downregulation of several LXR target genes involved in cholesterol homeostasis. This may lead to cholesterol accumulation within leukemic cells, responsible for high proliferative properties. We reported that LXR agonist treatment increases LXR target gene expression in BPDCN, stimulates cholesterol efflux from these cells, and is associated with the inhibition of proliferation and survival. These 2 effects may result from the interference of LXR activation with 2 BPDCN survival/proliferative pathways, namely IL-3 and NF-κB signaling pathways. The effects of LXR agonists are amplified by the addition of the lipid acceptor APOA1 known to enhance cholesterol efflux. All of these effects (except cell proliferation) were assessed in vitro in 2 BPDCN cell lines, expanded primary BPDCN cells, and several primary BPDCN samples isolated from 11 different patients. An in vivo therapeutic effect of LXR agonist is also observed in a xenograft model with reduction of BPDCN cell infiltration, prevention of BPDCN-induced cytopenia, and increased mouse survival. These data highlight an unrevealed perturbation of cholesterol homeostasis and LXR activity in BPDCN, and identify a new approach based on LXR agonists to treat this aggressive hematological malignancy.

Treatment of BPDCN with LXR agonists has several effects depending on their concentration. Restoration of LXR target gene expression (inducing cholesterol efflux) and inhibition of IL-3 and NF-κB signaling pathways occurred for concentrations between 1 and 10 μM (ranges usually used in malignant cells[10,38-42]). BPDCN cell proliferation (assessed with the proliferative BPDCN cell line, CAL-1) was significantly inhibited for 10 μM, as reported in several hematological malignancies and solid tumors.[39,42,43] Concentrations higher than 10 μM induced a significant BPDCN cell death, as reported for ovarian, breast, and colon cancer cells.[43-45] All of these data validate the concentrations of LXR agonists used in this study.

LXR activation in BPDCN triggers an apoptotic cell death mechanism based on different features, namely: exposure of phosphatidylserine (assessed by AnxV staining), cleavage of caspase-3 and caspase-9, as well as nucleus fragmentation. Induction of intrinsic apoptosis by LXR agonists was previously described in ovarian carcinoma cells,[45] and confirmed here associated with a significant increase of *BAX* and *BAK1* transcripts (encoding proapoptotic proteins). LXR-induced cell death in breast cancer cells has been demonstrated to implicate BAX upregulation and to be dependent on cholesterol efflux through ABCG1.[43] In our study, a stimulation of ABCA1/ABCG1-dependent cholesterol efflux via the addition of APOA1 increases LXR-mediated cytotoxic effects. APOA1-stimulated cholesterol efflux also potentiates the LXR-induced inhibition of Akt and STAT5 phosphorylation. This is in line with a previous report in prostate cancer cells showing Akt inhibition by increased cholesterol efflux.[10] Although exogenous APOA1 supplementation is required for in vitro assays with BPDCN cells, circulating lipid-free APOA1 (mainly produced by liver and intestine),[8] or APOA1 present in nascent HDL is likely to potentiate the impact of LXR agonist treatment in vivo. Overall, LXR stimulation in BPDCN exerts an antileukemic effect that can be enhanced by increasing cholesterol efflux.

Therapeutic strategies of BPDCN propose to interfere with IL-3[2,16,34,46] because BPDCNs express high levels of CD123,[2,26] and IL-3 is a BPDCN survival factor.[1,15] Here, we explored how LXR activation and LXR-induced cholesterol efflux interact with this pathway. No modification of CD131 and CD123 expression on BPDCN cells after LXR activation is observed (data not shown), whereas LXR agonists inhibit IL-3–induced Akt and STAT5 phosphorylation in BPDCN. Western blot analysis demonstrated that LXR agonists had no effect on STAT5 and Akt protein expression, suggesting a predominant effect at the phosphorylation levels.

BPDCN samples exhibit a specific downregulation of LXR target genes *ABCG1*, *ABCA1*, and *SREBF1*, in favor of repression of LXR transcriptomic activity. However, although LXR target gene transcription is decreased in BPDCN, the transcripts of the 2 LXR coding genes (*LXRA* and *LXRB*) are not and basal LXRβ protein (supplemental Figure 2B) is present. This suggests posttranscriptional regulation of LXR activity in BPDCN. LXR activity in normal PDC is inhibited by prior NF-κB activation.[25] Because NF-κB is constitutively activated in BPDCN,[32] and NF-κB p105 precursor-coding gene (*NFKB1*) is upregulated, LXR repression in BPDCN may be related to NF-κB activation. Restoration of the LXR pathway by agonist treatment in BPDCN inhibits the constitutive NF-κB activation at 3 different levels:

Figure 5 (continued) 3 BPDCN samples tested (LPDC #5, #6, #9). (C) CAL-1 and GEN2.2 cells were treated with increasing concentrations (12.5 μM, 25 μM, 50 μM, and 100 μM) of NF-κB inhibitor JSH23. Cell death was assessed by AnxV/7AAD staining, and analyzed by cytometry. Dot plots from 1 representative experiment of 5 and cumulative data from these 5 experiments expressed as percentage of dead AnxV$^+$ cells are shown (left panel). Cumulative data from 3 experiments expressed as mean ± SEM are shown (right panel) (**$P < .01$, Mann-Whitney). (D) Primary BPDCN cells were treated with 1 μM of LXR agonists for 24 hours, followed by 1 μg/mL of R848 for 45 minutes. P65 phosphorylation (pS536) was assessed by confocal microscopy. Data from 1 representative primary BPDCN sample of 4 (LPDC #5, #6, #8, #9) are shown. (E) CAL-1 cells were treated with 1 μM T0901317 (T09) or GW3965 (GW) for 24 hours, followed by R848 (1 μg/mL) stimulation for 6 hours. Cytosolic and nuclear protein fractions were isolated as described in "Methods". NF-κB1 (p105), p50, p65, and c-Rel proteins were analyzed by western blot and the expression of these proteins was compared with actin and lamin B expression (for cytosolic or nuclear expression, respectively) with the vehicle condition being considered as 1. Results from 1 representative experiment of 3.

Downloaded from http://ashpublications.net/blood/article-pdf/128/23/2694/1396962/blood724807.pdf by guest on 03 June 2024

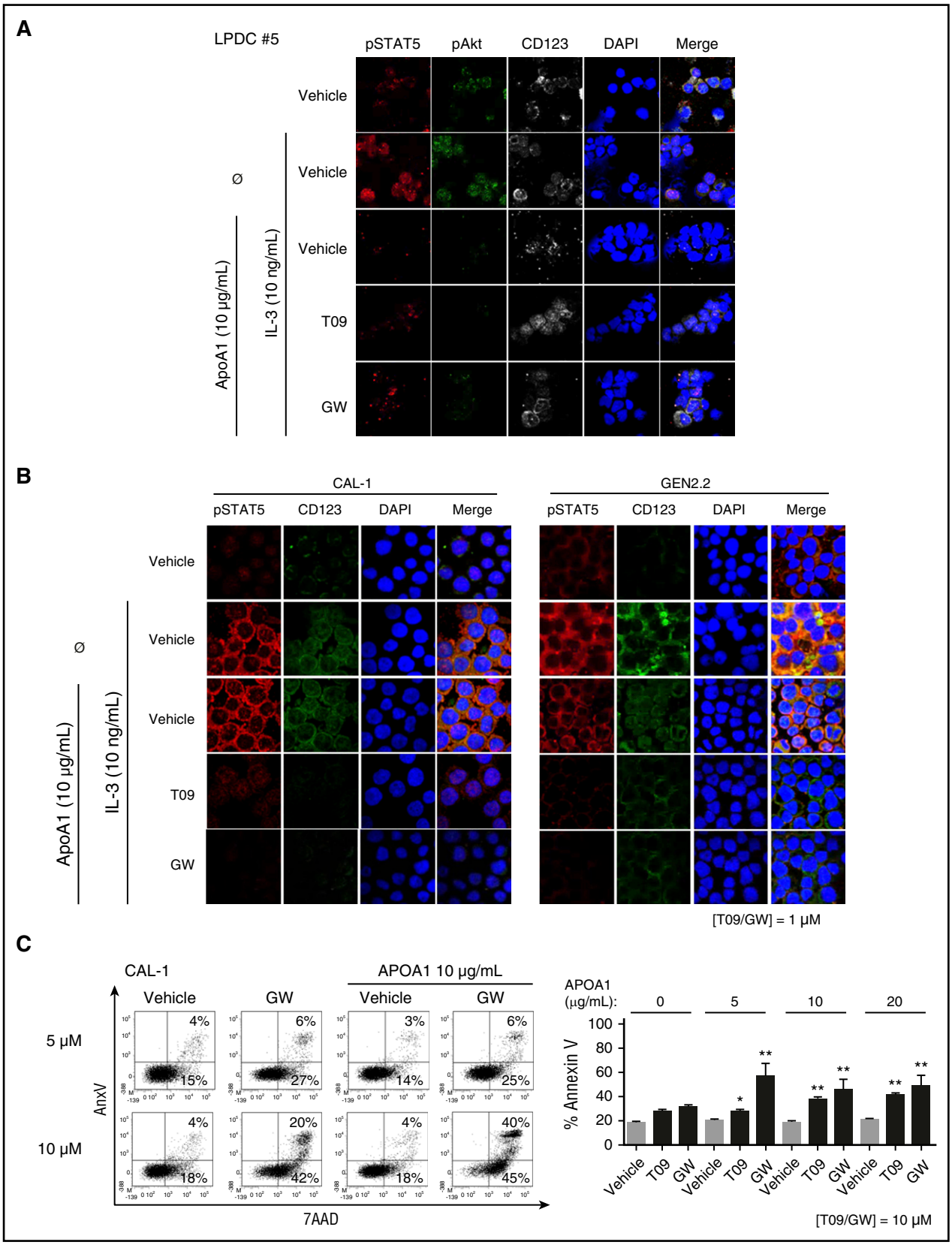

Figure 6. Cholesterol efflux stimulation in BPDCN cells amplifies LXR activation-induced effects. BPDCN CAL-1 and GEN2.2 cells or primary BPDCN samples were treated with 1 μM LXR agonists T0901317 (T09) or GW3965 (GW) for 24 hours. (A-B) Phospho-STAT5 (Y694) and phospho-Akt (S473) were assessed by confocal microscopy after LXR stimulation, followed by APOA1 (10 μg/mL) addition for 4 hours, and then IL-3 stimulation (10 ng/mL for 30 minutes). (A) Data from 1 representative sample of 2 BPDCN samples (LPDC #5, #8) are shown. (B) Data from 1 representative experiment of 3 for CAL-1 and GEN2.2 cells are shown. (C) CAL-1 cells were treated with 10 μM T0901317 or GW3965 simultaneously to increasing concentrations of APOA1 (5, 10, or 20 μg/mL) for 24 hours. Cell death was assessed by AnxV/7AAD staining analyzed by cytometry. Dot plots from 1 representative experiment of 6 are shown (left panel); only data obtained with GW treatment are depicted. Cumulative data from the 6 independent experiments expressed as mean ± SEM of dead AnxV$^+$ cells are shown (right panel, *$P < .05$, **$P < .01$, Mann-Whitney).

Downloaded from http://ashpublications.net/blood/article-pdf/128/23/2694/1396962/blood724807.pdf by guest on 03 June 2024

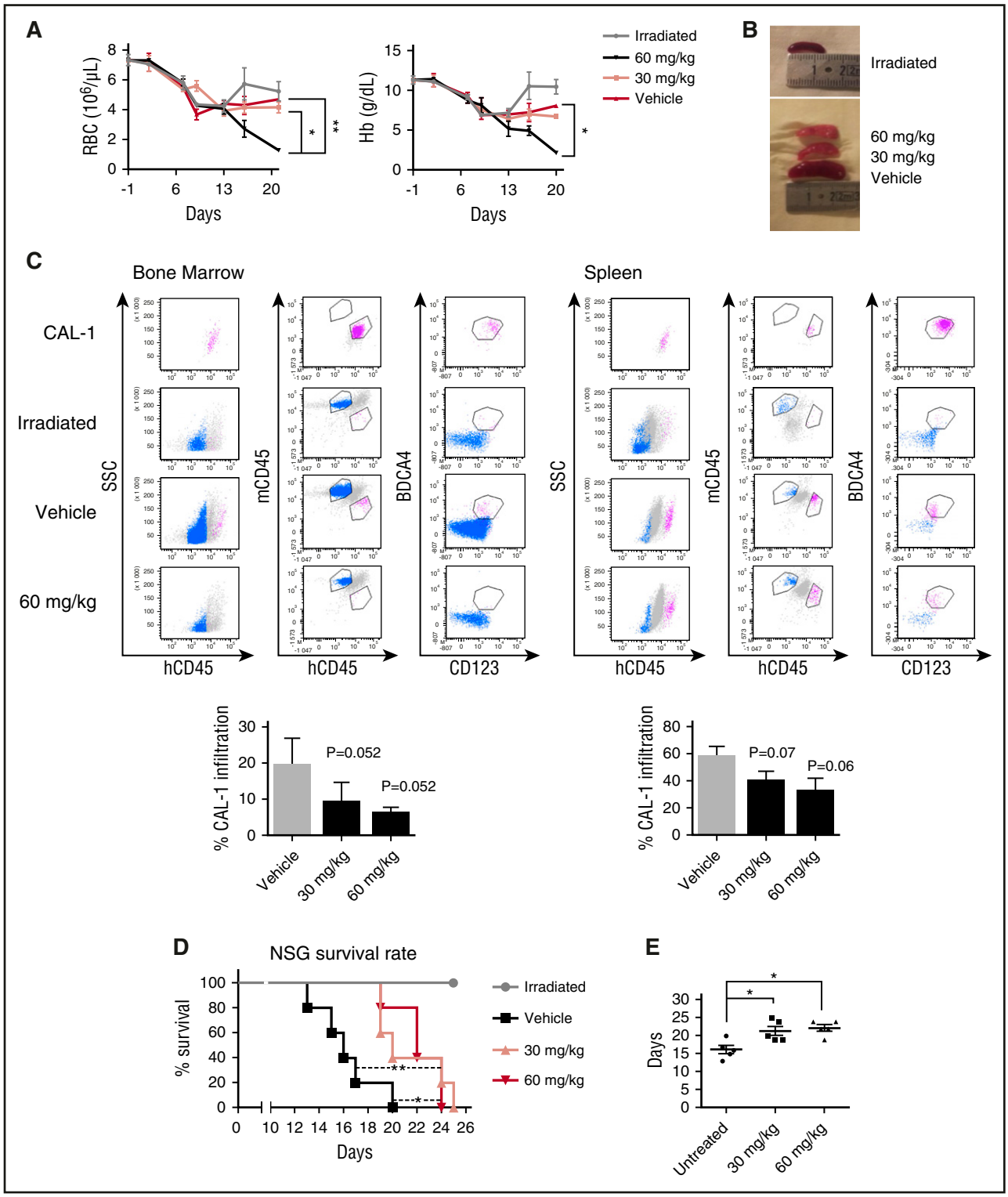

Figure 7. In vivo LXR agonist treatment limits BPDCN-induced cytopenia, spleen and bone marrow infiltration by BPDCN, and also improves overall mouse survival. NSG mice were sublethally irradiated (2 Gy), and then injected IV with 1×10^6 CAL-1 cells. After 7 days, mice were treated with 2 doses of the LXR agonist T0901317 (30 mg/kg or 60 mg/kg) or with vehicle control (PBS/DMSO 50%) every 2 days, until the end of the experiments (4 mice per group, 3 independent experiments). (A) Blood samples were collected every 4 days to assess RBC and Hb concentration. Cumulative data expressed as mean ± SEM are shown (*$P < .05$, **$P < .01$, Mann-Whitney). (B) At the end of the experiments (J20 ± 2), spleens were extracted and measured to evaluate BPDCN spleen involvement. (C) Spleens and bone marrow were collected in order to perform CAL-1 cell quantification. Cells were stained with the following antibodies: human CD45 (hCD45), murine CD45 (mCD45), CD123, and BDCA4 and analyzed by cytometry. Dot plots illustrate the gating strategy with identification of murine cells using mCD45 gating with irradiated mice used as control. Human CAL-1 cells were identified using hCD45, CD123, and BDCA4 staining. Cultured CAL-1 cells were used as control for this staining. Percentage of cell infiltration was calculated as follows: CAL-1 count/(hCD45 + mCD45 counts). Histograms represent cumulative data of 1 experiment of 3 expressed as mean ± SEM of CAL-1 cell infiltration percentage from 5 mice. (D) Overall survival of BPDCN-inoculated mice treated with LXR agonist T0901317 (30 mg/kg, pink triangles; 60 mg/kg, red triangles) or with vehicle (black squares). Irradiated mice (gray circles) were used as control. Statistical comparisons were performed between vehicle and treated groups using the Mantel-Cox test (*$P < .05$, **$P < .001$). (E) Mean overall survival of BPDCN-inoculated mice treated with LXR agonist or vehicle. Bars correspond to the mean of survival time (*$P < .05$, Mann-Whitney). Results from 1 additional experiment with 5 mice per group are shown.

Downloaded from http://ashpublications.net/blood/article-pdf/128/23/2694/1396962/blood724807.pdf by guest on 03 June 2024

p65 phosphorylation, nuclear translocation of the p50, p65, and cRel subunits, as well as transcription of *NFKB1* (data not shown). Our study confirms constitutive NF-κB activation in BPDCN cells,[32] and demonstrates that inhibition of p65 translocation by JSH-23 is sufficient to induce BPDCN cell death. This suggests that LXR agonist-induced cell death is related to NF-κB inhibition. Interestingly, STAT5 and NF-κB were also reported to promote G1 to S cell cycle phase transition through cyclin D1 induction, and thus cell proliferation.[47,48] In our study, BPDCN cells are retained in G1 phase after LXR activation. This suggests that LXR-induced STAT5 and NF-κB inhibition can be involved in both the inhibition of cell proliferation (through cell cycle arrest) and BPDCN cell death.

LXR agonist treatment of mice grafted with BPDCN cells prevents leukemia-induced cytopenia, reduces BPDCN spleen and bone marrow infiltrations, and slightly but significantly improves mouse survival. To date, the development of LXR agonists in clinical settings has been hampered by unwanted systemic side effects, such as fatty liver disease and LDL elevation.[19] Synthetic LXR agonists have been shown to exert therapeutic effects in mouse models of Alzheimer disease after oral administration.[19] This suggests that these agonists can cross the blood-brain barrier and may target BPDCN cells infiltrating the CNS. The CNS may represent a blast cell sanctuary in BPDCN patients with leukemic presentation both at diagnosis and at relapse.[4] Efforts are currently being made to generate new synthetic agonists with increased specificity for the LXRβ isoform, expressed by BPDCNs, to limit steatosis[19,49] and/or to stimulate LXR specifically in a target tissue.[50,51] Our study supports a new approach for BPDCN treatment using these new synthetic LXR agonists.

Acknowledgments

The authors thank T. Maeda (Nagasaki University, Japan) for kindly providing the BPDCN cell line CAL-1, J. Plumas and L. Chaperot for kindly providing the BPDCN cell line GEN2.2, W. Le Goff (INSERM UMR S1166, University "Pierre et Marie Curie", Paris, France) for helpful discussions on cholesterol metabolism, the Cytology laboratory of the Etablissement Français du Sang Bourgogne Franche-Comté (BFC), for blood cell and platelet counts, Sarah Odrion, and Alexis Varin for editorial assistance.

This work was supported by the Etablissement Français du Sang (grant 2011-11) (P.S.), the Agence Nationale de la Recherche (LabEx LipSTIC, ANR-11-LABX-0021), the Conseil Régional de Franche-Comté (soutien au LabEx LipSTIC 2015 and 2016) (P.S.), and the Fondation de Coopération Scientifique Bourgogne Franche-Comté (A.C., D.M., and P.S. via the Bonus Qualité Recherche BFC).

There are no current or pending patents related to this work. Two material transfer agreements related to the use of CAL-1 cell line and the GEN2.2 cell line are available.

Authorship

Contribution: A.C. performed most of the experiments, collected, assembled, and analyzed data, performed statistical analysis, and wrote the manuscript; D.M. performed cholesterol efflux experiments and helped to write the manuscript; A.R. and C.R. performed transcriptomic experiments and analysis; C.C. performed cell death analysis by flow cytometry, some immunoblotting, and qRT-PCR experiments; T.G. performed some confocal microscopy experiments; L.P. performed cell cycle experiments; B.L., F.A.-D., and F.B. performed and supported in vivo experiments; S.P. commented on the manuscript and helped to write it; S.B., C.P., and E.M. provided leukemia samples and diagnosis; L.L. commented on the manuscript and provided major funding support; F.G.-O. provided study material, collected data, and helped to write the manuscript; and P.S. supervised research, analyzed data, and wrote the manuscript.

Conflict-of-interest disclosure: The authors declare no competing financial interests.

The current affiliation for B.L. is Université Pierre et Marie Curie, UMR 938, INSERM, Paris, France.

ORCID profiles: P.S., 0000-0002-8857-9939.

Correspondence: Philippe Saas, EFS BFC, UMR 1098, INSERM, 8 rue JFX Girod, BP1937, F-25020 Besançon Cedex, France; e-mail: philippe.saas@efs.sante.fr.

References

1. Chaperot L, Bendriss N, Manches O, et al. Identification of a leukemic counterpart of the plasmacytoid dendritic cells. *Blood.* 2001;97(10):3210-3217.
2. Pemmaraju N. Blastic plasmacytoid dendritic cell neoplasm. *Clin Adv Hematol Oncol.* 2016;14(4):220-222.
3. Dalle S, Beylot-Barry M, Bagot M, et al. Blastic plasmacytoid dendritic cell neoplasm: is transplantation the treatment of choice? *Br J Dermatol.* 2010;162(1):74-79.
4. Martín-Martín L, Almeida J, Pomares H, et al. Blastic plasmacytoid dendritic cell neoplasm frequently shows occult central nervous system involvement at diagnosis and benefits from intrathecal therapy. *Oncotarget.* 2016;7(9):10174-10181.
5. Pileri A, Delfino C, Grandi V, Agostinelli C, Pileri SA, Pimpinelli N. Blastic plasmacytoid dendritic cell neoplasm (BPDCN): the cutaneous sanctuary. *G Ital Dermatol Venereol.* 2012;147(6):603-608.
6. Vitols S, Norgren S, Juliusson G, Tatidis L, Luthman H. Multilevel regulation of low-density lipoprotein receptor and 3-hydroxy-3-methylglutaryl coenzyme A reductase gene expression in normal and leukemic cells. *Blood.* 1994;84(8):2689-2698.
7. Tatidis L, Gruber A, Vitols S. Decreased feedback regulation of low density lipoprotein receptor activity by sterols in leukemic cells from patients with acute myelogenous leukemia. *J Lipid Res.* 1997;38(12):2436-2445.
8. Oram JF, Vaughan AM. ATP-binding cassette cholesterol transporters and cardiovascular disease. *Circ Res.* 2006;99(10):1031-1043.
9. Ikonen E. Cellular cholesterol trafficking and compartmentalization. *Nat Rev Mol Cell Biol.* 2008;9(2):125-138.
10. Pommier AJ, Alves G, Viennois E, et al. Liver X receptor activation downregulates AKT survival signaling in lipid rafts and induces apoptosis of prostate cancer cells. *Oncogene.* 2010;29(18):2712-2723.
11. Singh P, Saxena R, Srinivas G, Pande G, Chattopadhyay A. Cholesterol biosynthesis and homeostasis in regulation of the cell cycle. *PLoS One.* 2013;8(3):e58833.
12. Sun Y, Sukumaran P, Varma A, Derry S, Sahmoun AE, Singh BB. Cholesterol-induced activation of TRPM7 regulates cell proliferation, migration, and viability of human prostate cells. *Biochim Biophys Acta.* 2014;1843(9):1839-1850.
13. Yvan-Charvet L, Pagler T, Gautier EL, et al. ATP-binding cassette transporters and HDL suppress hematopoietic stem cell proliferation. *Science.* 2010;328(5986):1689-1693.
14. Murphy AJ, Akhtari M, Tolani S, et al. ApoE regulates hematopoietic stem cell proliferation, monocytosis, and monocyte accumulation in atherosclerotic lesions in mice. *J Clin Invest.* 2011;121(10):4138-4149.
15. Garnache-Ottou F, Chaperot L, Biichle S, et al. Expression of the myeloid-associated marker CD33 is not an exclusive factor for leukemic plasmacytoid dendritic cells. *Blood.* 2005;105(3):1256-1264.
16. Frankel AE, Woo JH, Ahn C, et al. Activity of SL-401, a targeted therapy directed to interleukin-3 receptor, in blastic plasmacytoid dendritic cell neoplasm patients. *Blood.* 2014;124(3):385-392.
17. Pemmaraju N, Lane AA, Sweet KL, et al. Results from phase 2 registration trial of SL-401 in patients with blastic plasmacytoid dendritic cell neoplasm (BPDCN): lead-in completed,

Downloaded from http://ashpublications.net/blood/article-pdf/128/23/2694/1396962/blood724807.pdf by guest on 03 June 2024

expansion satge ongoing [abstract]. *J Clin Oncol.* 2016;34(15 suppl). Abstract 7006.

18. Im SS, Osborne TF. Liver x receptors in atherosclerosis and inflammation. *Circ Res.* 2011;108(8):996-1001.
19. Hong C, Tontonoz P. Liver X receptors in lipid metabolism: opportunities for drug discovery. *Nat Rev Drug Discov.* 2014;13(6):433-444.
20. Lin CY, Gustafsson JA. Targeting liver X receptors in cancer therapeutics. *Nat Rev Cancer.* 2015;15(4):216-224.
21. Wójcicka G, Jamroz-Wiśniewska A, Horoszewicz K, Bełtowski J. Liver X receptors (LXRs). Part I: structure, function, regulation of activity, and role in lipid metabolism. *Postepy Hig Med Dosw (Online).* 2007;61:736-759.
22. Dove DE, Linton MF, Fazio S. ApoE-mediated cholesterol efflux from macrophages: separation of autocrine and paracrine effects. *Am J Physiol Cell Physiol.* 2005;288(3):C586-C592.
23. Hong C, Duit S, Jalonen P, et al. The E3 ubiquitin ligase IDOL induces the degradation of the low density lipoprotein receptor family members VLDLR and ApoER2. *J Biol Chem.* 2010;285(26): 19720-19726.
24. Zhang L, Reue K, Fong LG, Young SG, Tontonoz P. Feedback regulation of cholesterol uptake by the LXR-IDOL-LDLR axis. *Arterioscler Thromb Vasc Biol.* 2012;32(11):2541-2546.
25. Ceroi A, Delettre FA, Marotel C, et al. The anti-inflammatory effects of platelet-derived microparticles in human plasmacytoid dendritic cells involve liver X receptor activation. *Haematologica.* 2016;101(3):e72-e76.
26. Garnache-Ottou F, Feuillard J, Ferrand C, et al; GOELAMS and GEIL study. Extended diagnostic criteria for plasmacytoid dendritic cell leukaemia. *Br J Haematol.* 2009;145(5):624-636.
27. Angelot-Delettre F, Biichle S, Ferrand C, et al. Intracytoplasmic detection of TCL1–but not ILT7- by flow cytometry is useful for blastic plasmacytoid dendritic cell leukemia diagnosis. *Cytometry A.* 2012;81(8):718-724.
28. Riaz W, Zhang L, Horna P, Sokol L. Blastic plasmacytoid dendritic cell neoplasm: update on molecular biology, diagnosis, and therapy. *Cancer Contr.* 2014;21(4):279-289.
29. Maeda T, Murata K, Fukushima T, et al. A novel plasmacytoid dendritic cell line, CAL-1, established from a patient with blastic natural killer cell lymphoma. *Int J Hematol.* 2005;81(2): 148-154.
30. Chaperot L, Blum A, Manches O, et al. Virus or TLR agonists induce TRAIL-mediated cytotoxic activity of plasmacytoid dendritic cells. *J Immunol.* 2006;176(1):248-255.
31. Ishibashi M, Filomenko R, Rébé C, et al. Knock-down of the oxysterol receptor LXRα impairs cholesterol efflux in human primary macrophages: lack of compensation by LXRβ activation. *Biochem Pharmacol.* 2013;86(1):122-129.
32. Sapienza MR, Fuligni F, Agostinelli C, et al; AIRC 5xMille consortium 'Genetics-driven targeted management of lymphoid malignancies and the Italian Registry on Blastic Plasmacytoid Dendritic Cell Neoplasm. Molecular profiling of blastic plasmacytoid dendritic cell neoplasm reveals a unique pattern and suggests selective sensitivity to NF-kB pathway inhibition. *Leukemia.* 2014; 28(8):1606-1616.
33. Reddy EP, Korapati A, Chaturvedi P, Rane S. IL-3 signaling and the role of Src kinases, JAKs and STATs: a covert liaison unveiled. *Oncogene.* 2000;19(21):2532-2547.
34. Testa U, Pelosi E, Frankel A. CD 123 is a membrane biomarker and a therapeutic target in hematologic malignancies. *Biomark Res.* 2014; 2(1):4.
35. Zhuang J, Hawkins SF, Glenn MA, et al. Akt is activated in chronic lymphocytic leukemia cells and delivers a pro-survival signal: the therapeutic potential of Akt inhibition. *Haematologica.* 2010; 95(1):110-118.
36. Schafranek L, Nievergall E, Powell JA, et al. Sustained inhibition of STAT5, but not JAK2, is essential for TKI-induced cell death in chronic myeloid leukemia. *Leukemia.* 2015;29(1):76-85.
37. Zidovetzki R, Levitan I. Use of cyclodextrins to manipulate plasma membrane cholesterol content: evidence, misconceptions and control strategies. *Biochim Biophys Acta.* 2007;1768(6): 1311-1324.
38. Vedin LL, Lewandowski SA, Parini P, Gustafsson JA, Steffensen KR. The oxysterol receptor LXR inhibits proliferation of human breast cancer cells. *Carcinogenesis.* 2009;30(4):575-579.
39. Vedin LL, Gustafsson JA, Steffensen KR. The oxysterol receptors LXRα and LXRβ suppress proliferation in the colon. *Mol Carcinog.* 2013; 52(11):835-844.
40. Geyeregger R, Shehata M, Zeyda M, et al. Liver X receptors interfere with cytokine-induced proliferation and cell survival in normal and leukemic lymphocytes. *J Leukoc Biol.* 2009;86(5): 1039-1048.
41. Sanchez PV, Glantz ST, Scotland S, Kasner MT, Carroll M. Induced differentiation of acute myeloid leukemia cells by activation of retinoid X and liver X receptors. *Leukemia.* 2014;28(4):749-760.
42. Agarwal JR, Wang Q, Tanno T, et al. Activation of liver X receptors inhibits hedgehog signaling, clonogenic growth, and self-renewal in multiple myeloma. *Mol Cancer Ther.* 2014;13(7): 1873-1881.
43. El Roz A, Bard JM, Huvelin JM, Nazih H. LXR agonists and ABCG1-dependent cholesterol efflux in MCF-7 breast cancer cells: relation to proliferation and apoptosis. *Anticancer Res.* 2012; 32(7):3007-3013.
44. Derangère V, Chevriaux A, Courtaut F, et al. Liver X receptor β activation induces pyroptosis of human and murine colon cancer cells. *Cell Death Differ.* 2014;21(12):1914-1924.
45. Rough JJ, Monroy MA, Yerrum S, Daly JM. Anti-proliferative effect of LXR agonist T0901317 in ovarian carcinoma cells. *J Ovarian Res.* 2010;3:13.
46. Angelot-Delettre F, Roggy A, Frankel AE, et al. In vivo and in vitro sensitivity of blastic plasmacytoid dendritic cell neoplasm to SL-401, an interleukin-3 receptor targeted biologic agent. *Haematologica.* 2015;100(2):223-230.
47. Dagvadorj A, Kirken RA, Leiby B, Karras J, Nevalainen MT. Transcription factor signal transducer and activator of transcription 5 promotes growth of human prostate cancer cells in vivo. *Clin Cancer Res.* 2008;14(5):1317-1324.
48. Hinz M, Krappmann D, Eichten A, Heder A, Scheidereit C, Strauss M. NF-kappaB function in growth control: regulation of cyclin D1 expression and G0/G1-to-S-phase transition. *Mol Cell Biol.* 1999;19(4):2690-2698.
49. Kirchgessner TG, Martin R, Sleph P, et al. Pharmacological characterization of a novel liver X receptor agonist with partial LXRα activity and a favorable window in nonhuman primates. *J Pharmacol Exp Ther.* 2015;352(2):305-314.
50. Hu B, Unwalla RJ, Goljer I, et al. Identification of phenylsulfone-substituted quinoxaline (WYE-672) as a tissue selective liver X-receptor (LXR) agonist. *J Med Chem.* 2010;53(8):3296-3304.
51. Lim RK, Yu S, Cheng B, et al. Targeted delivery of LXR agonist using a site-specific antibody-drug conjugate. *Bioconjug Chem.* 2015;26(11): 2216-2222.

Downloaded from http://ashpublications.net/blood/article-pdf/128/23/2694/1396962/blood724807.pdf by guest on 03 June 2024